



The preparation of the α -iodo-substituted tripods within the series of tris(2-pyridylmethyl)amine ligands, and the characterization of the corresponding $I_{1-3}TPAFeCl_2$ complexes

Hassen Jaafar, Rémy Louis, Dominique Mandon*

Laboratoire de Chimie Biomimétique des Métaux de Transition, UMR CNRS n° 7177, Institut de Chimie et Université de Strasbourg, Bâtiment Le Bel, 4 rue Blaise Pascal, F-67070 Strasbourg cedex, France

ARTICLE INFO

Article history:

Received 22 June 2010

Received in revised form 14 October 2010

Accepted 22 October 2010

Available online 28 October 2010

Keywords:

Halogen-substituted tris(2-pyridylmethyl)amine ligands
Iron complexes
Tripodal tetraamines

ABSTRACT

We report in this communication the easy preparation of the α -iodo substituted tripods within the series of tris(2-pyridylmethyl)amine ligands, I_1TPA , I_2TPA and I_3TPA , respectively. The characterization of the corresponding $FeCl_2$ complexes in solution is described and structural analysis by X-ray diffraction for $I_1TPAFeCl_2$ and $I_2TPAFeCl_2$ is also reported. The steric effect of the iodo substituent is evidenced: (i) by elongation of the metal to iodo-pyridine distance within $I_1TPAFeCl_2$, which however remains a very stable compound; (ii) by decoordination of one substituted pyridine in $I_2TPAFeCl_2$ and $I_3TPAFeCl_3$. In $I_2TPAFeCl_2$ and in the solid state, this uncoordinated pyridine strongly interacts with the same fragment of the neighbouring molecule, providing an overall dinuclear arrangement for this complex.

© 2010 Elsevier B.V. All rights reserved.

1. Introduction

The inorganic chemistry of tripodal ligands based on the tris(2-pyridylmethyl)amine (TPA) motif has, over the last 20 years, undergone a tremendous development: these small tetraamine ligands are easy to prepare, coordinate most metal ions of the periodic table yielding stable complexes, and therefore find potential application in many research areas [1–3].

Iron complexes with TPA-type tripods have been used as powerful tools to understand the structure/function relationship at active sites of non-heme iron proteins in which the metal centres have high-valent oxidation states [4,5]. Complexes with α -substituted tris(2-pyridylmethyl)amine ligands have also been used as platforms to address reactivity questions such as coordination of dioxygen to Fe^{II} centres [6–9], or intramolecular conversion of various functional groups [9–11]. In terms of properties, it has already been shown that TPA-type tripods can be considered as borderline ligands with respect to the ligand field they provide to metal complexes: this is particularly true with ferric hydroperoxides, for which a change in the spin state is observed upon methyl substitution of the tripod [12]. In relation to this point, an other important investigation area for which α -substitution of TPA ligands might be extremely useful is the question of spin conversions in metal

complexes. Exogenous ligands such as thiocyanate [13], cyanides [14–16], nitrogen-containing bridging ligands [16] or catecholates [17–19] to cite only a few recent examples, once coordinated to the metal centre in TPA complexes, yield compounds which undergo spin conversions. Keeping this in mind, the control of the electronic and steric properties within this kind of tripodal ligands appears to be highly desirable, and substitution of the pyridine units represents an easy way to achieve this goal.

Whereas alkyl substitution at the α position was described shortly after the first report of the synthesis of the parent tripod [20–23], halide substitution appeared more recently, with bromine atoms first [24], followed by chloride¹ and fluoride [8,25] substituents. Surprisingly, there was no mention of any α -substituted tripods with iodine, despite the fact that this atom displays the biggest atomic radius within the commonly referred series of stable halogens (F, Cl, Br and I), making from these tripods interesting candidates to address the dichotomic question of electronic versus steric effects in coordination chemistry.

The goal of the present article is to makeup this lack of information by reporting the preparation of the series of α -iodo-substituted TPA tripods, as well as the spectroscopic properties of the corresponding $FeCl_2$ complexes, and the crystal structures of two of them, $I_1TPAFeCl_2$ and $I_2TPAFeCl_2$, respectively.

* Corresponding author. Tel.: +33 (0)368 851 537; fax: +33 (0)368 851 438.
E-mail address: mandon@chimie.u-strasbg.fr (D. Mandon).

¹ For the mono α -chlorosubstituted tripod, see Ref. [23]. The preparation of di- and tris- α -chlorosubstituted ligands will be reported in a forthcoming article from this laboratory.

2. Experimental

2.1. General considerations and physical methods

All solvents used during the metallation reactions and work-up were distilled and dried according to published procedures [26] and degassed shortly before use. 2-aminomethyl pyridine, trimethylsilyl chloride and sodium iodide were purchased from Aldrich and used as received. Analytical anhydrous FeCl_2 was obtained as a white powder by reacting iron powder (ACS grade) with hydrochloric acid in the presence of methanol under an argon atmosphere. 2-Bromo-6-methylpyridine [27] and bis(2-pyridylmethyl)amine (DPA) [21] were prepared as previously reported. 2-Iodo-6-methylpyridine was prepared according to an already published procedure [31]. UV–Vis spectra were recorded on a Varian Cary 05e UV–Vis–NIR spectrophotometer at room temperature in CH_3CN . ^1H NMR data were collected in CD_3CN solutions (or CDCl_3 for free ligands) on a Bruker AC 300 spectrometer at 300.1300 MHz using the residual signal of CD_2HCN (CHCl_3 for ligand) as a reference for calibration. Conductivity measurements were carried out under argon at 20 °C with a CDM 210 Radiometer Copenhagen Conductivity Meter, using a Tacussel CDC745-9 electrode. Cyclic voltammetry measurements were obtained from a PAR 273A potentiostat in a 0.1 M acetonitrile solution of TBAPF₆ (supporting electrolyte), using platinum electrodes and saturated calomel electrode as reference. For each measurement, the potential was checked by addition of a small amount of ferrocene ($\text{Fc}/\text{Fc}^+ = 0.380 \text{ V}/\text{SCE}$) in the cell. Elemental analyses were carried out by the Service Central d'Analyses de l'Institut de Chimie de Strasbourg. Mass spectra were obtained from the Service de Spectrométrie de Masse de l'Institut de Chimie de Strasbourg.

2.2. Syntheses

2.2.1. Ligands

2-(Bromomethyl)-6-iodopyridine: To a solution of 4 g, (18.2 mmol) of 2-iodo-6-methyl pyridine in 200 cm³ of CCl_4 were added 3.6 g (20 mmol) of N-bromosuccinimide, and 180 mg (0.7 mmol) of dibenzoyl peroxide. The medium was refluxed for 5 h, then cooled to room temperature. The solvent was evaporated, and the residue extracted with toluene. After filtration, the toluene solution was washed with water, and dried on MgSO_4 . The concentrated toluene phase was deposited at the top of a chromatography column mounted with silicagel/toluene. Elution using toluene afforded the desired compound as the third fraction. 1.44 g (4.8 mmol) of a white solid were obtained, corresponding to a 26.5% yield of 2-iodo 6-bromomethyl pyridine.

^1H NMR (CDCl_3), δ , ppm: 7.64 (d, 1H); 7.43 (d, 1H); 7.32 (t, 1H), 4.48 (s, 2H).

$\text{I}_1\text{TPA} = (2\text{-iodo } 6\text{-pyridylmethyl})\text{bis}(2\text{-pyridylmethyl})\text{amine}$: To a solution of 0.5 g (1.67 mmol) of 2-(bromomethyl)-6-iodopyridine in 200 cm³ of EtOH were added 0.33 g (1.65 mmol) of bis(2-pyridylmethyl)amine and 0.85 g (0.01 mmol) of NaHCO_3 . The reaction mixture was refluxed over 16 h. Afterwards, the solvent was evaporated to dryness. Water was then added, and the mixture was extracted several times with CH_2Cl_2 . The combined organic phases were washed with water then dried over MgSO_4 . Addition of pentane to the concentrated organic phases allowed precipitation of a white solid, which was filtered and dried under vacuum. Obtained: 0.28 g, corresponding to a 43.5% yield.

^1H NMR, CDCl_3 , δ , ppm: 8.54 (m, $\alpha\text{-CH}_{\text{arom}}$, 2H); 7.70–7.50 (m, CH_{arom} , 6H); 7.28 (t, CH_{arom} , 1H); 7.15 (m, CH_{arom} , 2H); 3.89, (s, CH_2 , 4H); 3.87 (s, CH_2 , 2H). The spectrum is displayed in the [Supplementary Content](#) section.

Elemental Anal. Calc. for $\text{C}_{18}\text{H}_{17}\text{N}_4\text{I}$: C, 51.9; H, 4.1; N, 13.4. Found: C, 51.7; H, 4.2; N, 13.3%.

$\text{I}_2\text{TPA} = \text{bis}(2\text{-iodo-6-pyridylmethyl})(2\text{-pyridylmethyl})\text{amine}$: To a solution of 0.5 g (1.67 mmol) of 2-(bromomethyl)-6-iodopyridine in 200 cm³ of EtOH were added 0.09 g (0.83 mmol) of picolylamine and 1.2 g (10.00 mmol) of Na_2CO_3 . The reaction mixture was refluxed over 16 h. Afterwards, the solvent was evaporated to dryness. Water was then added and the mixture was extracted several times with CH_2Cl_2 . The combined organic phases were washed with water then dried over MgSO_4 . The concentrated solution was deposited at the top of a chromatographic column mounted with silicagel/diethyl ether. The column was washed with diethyl ether, and the desired ligand was obtained upon elution with a 50:50 mixture of diethyl ether and acetone. Concentration afforded 0.26 g of a white solid, corresponding to a 30% yield.

^1H NMR, CDCl_3 , δ , ppm: 8.53 (m, $\alpha\text{-CH}_{\text{arom}}$, 1H); 7.70–7.50 (m, CH_{arom} , 6H); 7.28 (t, CH_{arom} , 1H); 7.15 (m, CH_{arom} , 1H); 3.88, (s, CH_2 , 2H); 3.85 (s, CH_2 , 4H). The spectrum is displayed in the [Supplementary Content](#) section.

Elemental Anal. Calc. for $\text{C}_{18}\text{H}_{16}\text{N}_4\text{I}_2$: C, 39.8; H, 2.9; N, 10.3. Found: C, 39.7; H, 3.3; N, 10.0%.

$\text{I}_3\text{TPA} = \text{tris}(2\text{-iodo-6-pyridylmethyl})\text{amine}$: 1.45 g (4.8 mmol) of 2-(bromomethyl)-6-iodopyridine were suspended with NH_4Cl (96 mg, 1.60 mmol) in a mixture THF/ H_2O 90:10 (150 cm³). The pH was raised by addition of aqueous NaOH until a value of 10 was readable after having spotted the medium on a pH paper. The resulting medium was stirred 4 days at room temperature in a tightly closed flask. After THF evaporation, the reaction mixture was then poured into CH_2Cl_2 and the organic phase separated, washed with water and then dried by MgSO_4 . Addition of cold hexane to the concentrated organic phases yielded 0.63 g (58%) of a white solid.

^1H NMR, CDCl_3 , δ , ppm: 7.60–7.50 (m, CH_{arom} , 6H); 7.28 (t, CH_{arom} , 3H); 3.85 (s, CH_2 , 6H). The spectrum is displayed in the [Supplementary Content](#) section.

Elemental Anal. Calc. for $\text{C}_{18}\text{H}_{15}\text{N}_4\text{I}_3$: C, 32.3; H, 2.2; N, 8.3. Found: C, 32.4; H, 2.7; N, 8.2%.

2.2.2. Complexes

Preparation and handling of the complexes were performed under argon atmosphere by using Schlenk technique following standard procedures [28].

Details are given for $\text{I}_1\text{TPAFeCl}_2$, but the following procedure applies to all complexes: 150 mg (0.36 mmol) of free I_1TPA were dissolved in a schlenk tube containing 20 cm³ of dry and degassed THF. 46 mg (0.36 mmol) of anhydrous FeCl_2 was dissolved in a second schlenk tube containing 10 cm³ of dry and degassed THF. The solution of FeCl_2 was transferred under argon in the schlenk containing the ligand, and the medium was stirred overnight. The solvent was then evaporated to dryness, and the compound was extracted with dry and degassed CH_3CN , filtered under inert atmosphere and concentrated. Addition of diethyl ether afforded a yellow solid, which was washed thoroughly with this solvent, prior to be dried under vacuum. 160 mg (82%) of $\text{I}_1\text{TPAFeCl}_2$ with good spectroscopic data could be obtained. Additional washings with a mixture of diethyl ether/ CH_2Cl_2 followed by an other evaporation cycle is sometimes necessary to get rid of unreacted free ligand.

Single crystals were obtained by slow diffusion of diethyl ether in a sealed tube containing $\text{I}_1\text{TPAFeCl}_2$ in solution in CH_3CN , and I_2FeCl_2 in solution in CH_2Cl_2 . The crystals obtained by this way were crushed and dissolved in dry and degassed acetonitrile, and the spectroscopic data (UV–Vis and ^1H NMR) of the solution were found to be identical to those obtained from the powder samples. $\text{I}_1\text{TPAFeCl}_2$: UV–Vis, CH_3CN , R.T., λ , nm ($10^3 \text{ mol}^{-1} \text{ L cm}^{-1}$): 258 (5.5); 375 (1.0).

^1H NMR, CD_3CN , δ , ppm, ($\Delta\nu_{1/2}$, Hz): 117, α (553); 67, 57, 42, CH_2 (608, 352, 521); 51, 46, β , β' unsubst.Py (40, 42); 28, 18, β , β' subst.Py (87, 150); 10, γ unsubstPy (28); 8, γ substPy (24). Assignment realized by

comparison with the already well known BrTPAFeCl_2 complex, for which a qualitatively similar spectrum is reported in Ref. [28].

Elemental Anal. Calc. for $\text{C}_{18}\text{H}_{17}\text{N}_4\text{I}_2\text{FeCl}_2 \cdot \frac{1}{2} \text{CH}_2\text{Cl}_2$: C, 37.9; H, 3.1; N, 9.5. Found: C, 38.1; H, 3.5; N, 9.8%.

Cyclic voltammetry, CH_3CN TBAPF₆ 0.1 M, 200 mV/s $C = 3$ mMol: $E_{1/2\text{Fe(II)Fe(III)}} = 210$ mV/SCE. $\Delta E_{\text{c/Ea}} = 190$ mV. $I_{\text{pc}}/I_{\text{pa}} = 0.91$.

Molecular conductivity, 3.7 mMol, CH_3CN : $\Lambda = 19.2$ S $\text{cm}^2 \text{mol}^{-1}$.

$\text{I}_2\text{TPAFeCl}_2$: UV–Vis, CH_3CN , R.T., λ , nm ($10^3 \text{mol}^{-1} \text{L cm}^{-1}$): 246 (7.1); 370 (0.5).

^1H NMR, CD_3CN , δ , ppm ($\Delta_{\text{v1/2}}$, Hz): 121, α (680); 88, 74, 47, CH_2 (920, 700, 670); 55, 32, 19, β , β' (90, 265, 333).

Elemental Anal. Calc. for $\text{C}_{18}\text{H}_{16}\text{N}_4\text{I}_2\text{FeCl}_2$: C, 32.3; H, 2.4; N, 8.4. Found: C, 32.7; H, 2.7; N, 8.3%.

Cyclic voltammetry, CH_3CN TBAPF₆ 0.1 M, 200 mV/s $C = 2.5$ mMol: $E_{1/2\text{Fe(II)Fe(III)}} = 44$ mV/SCE. $\Delta E_{\text{c/Ea}} = 150$ mV. $I_{\text{pc}}/I_{\text{pa}} = 0.85$.

Molecular conductivity, 3.4 mMol, CH_3CN : $\Lambda = 23.1$ S $\text{cm}^2 \text{mol}^{-1}$.

$\text{I}_3\text{TPAFeCl}_2$: UV–Vis, CH_3CN , R.T., λ , nm ($10^3 \text{mol}^{-1} \text{L cm}^{-1}$): 276 (14.3). No MLCT absorption.

^1H NMR, CD_3NO_2 , δ , ppm, ($\Delta_{\text{v1/2}}$, Hz): Poor solubility. No tractable signals detected.

Mass Spectroscopy: esi positive, m/z : found: 758.729 (100%), 759.726 (22%), 760.727 (32%), perfectly matching the cluster $[\text{C}_{18}\text{H}_{15}\text{N}_4\text{I}_3\text{FeCl}]^+$, $[\text{I}_3\text{TPAFeCl}]^+$ for which the calculated values are: 758.746 (100%), 759.749 (22%), 760.744 (31.5%).

Elemental Anal. Calc. for $\text{C}_{18}\text{H}_{15}\text{N}_4\text{I}_3\text{FeCl}_2 \cdot \text{CH}_2\text{Cl}_2$: C, 25.9; H, 1.9; N, 6.4. Found: C, 25.9; H, 2.2; N, 6.6%.

Cyclic voltammetry, CH_3CN TBAPF₆ 0.1 M, 200 mV/s $C = \text{saturation}$: $E_{1/2\text{Fe(II)Fe(III)}} = 54$ mV/SCE. $\Delta E_{\text{c/Ea}} = 170$ mV. $I_{\text{pc}}/I_{\text{pa}} = 0.93$.

Molecular conductivity, 1.0 mMol, CH_3CN : $\Lambda = 15.3$ S $\text{cm}^2 \text{mol}^{-1}$.

2.3. Crystal structures

Single crystals were obtained by slow diffusion of diethyl ether in a sealed tube containing $\text{I}_1\text{TPAFeCl}_2$ in solution in CH_3CN , and I_2FeCl_2 in solution in CH_2Cl_2 .

Selected single crystal was mounted on a Nonius Kappa-CCD area detector diffractometer (Mo $\text{K}\alpha$ $\lambda = 0.71073$ Å). The complete conditions of data collection (DENZO software [29]) and structure

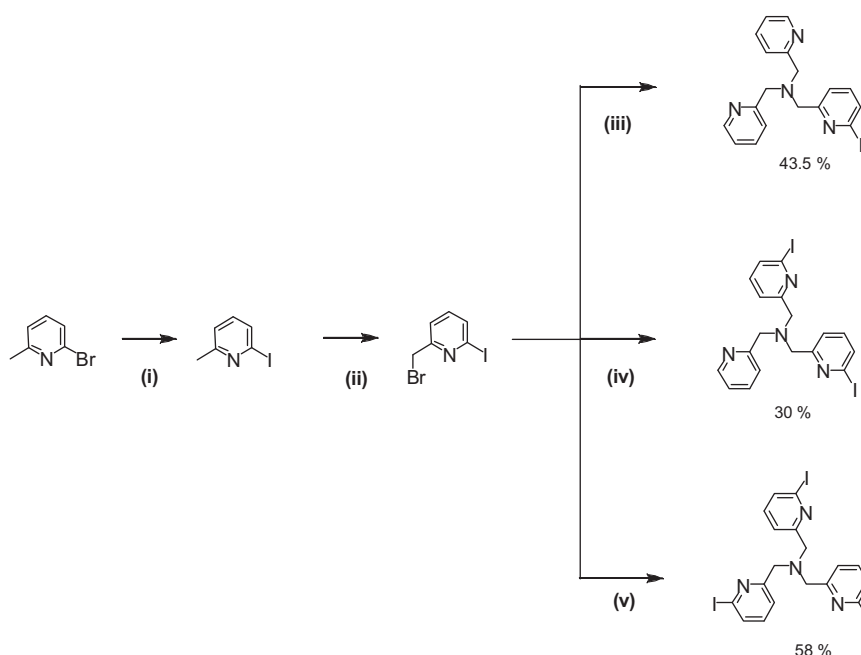
refinements are given below. The cell parameters were determined from reflections taken from one set of 10 frames (1.0° steps in phi angle), each at 20 s exposure. The structures were solved using direct methods (SHELXS97) and refined against F^2 using the SHELXL97 software [30]. No absorption correction was applied. All non-hydrogen atoms were refined anisotropically. Hydrogen atoms were generated according to stereochemistry and refined using a riding model in SHELXL97. The R_2 value refers to all data; the R_1 value refers to observed data.

$\text{I}_1\text{TPAFe}^{(\text{II})}\text{Cl}_2 = \text{C}_{18}\text{H}_{17}\text{C}_{12}\text{FeI}_2\text{N}_4$, $T = 173$ (2) K, M.W. = 543.01. Triclinic, $P\bar{1}$, $a = 8.9812(3)$ Å, $b = 13.7106(3)$ Å, $c = 16.7178(7)$ Å, $\alpha = 92.518(2)^\circ$, $\beta = 105.340(1)^\circ$, $\gamma = 92.663(2)^\circ$, $V = 1979.73(12)$ Å³. $D_{\text{calc}} = 1.822$ g cm^{-3} , $Z = 4$, $R_1 = 0.0415$, $wR_2 = 0.1216$ for 9005 reflections, θ max = 27.47° . $R_{\text{int}} = 0.0450$, total number of reflexions: 20356.

$\text{I}_2\text{TPAFe}^{(\text{II})}\text{Cl}_2 = \text{C}_{18}\text{H}_{16}\text{C}_{12}\text{FeI}_2\text{N}_4$, CH_2Cl_2 , $T = 173$ (2) K, M.W. = 753.82. Monoclinic, $P2_1/c$, $a = 8.1785(2)$ Å, $b = 15.2004(5)$ Å, $c = 21.2058(6)$ Å, $\beta = 106.957(2)^\circ$, $V = 2521.62(13)$ Å³. $D_{\text{calc}} = 1.986$ g cm^{-3} , $Z = 4$, $R_1 = 0.0546$, $wR_2 = 0.1719$ for 5577 reflections, θ max = 27.5° . $R_{\text{int}} = 0.0557$, total number of reflexions: 14949.

3. Results and discussion

Synthesis of tris(2-pyridylmethyl)amine (TPA) – type ligands is generally achieved following two alternative pathways: (i) the condensation of 2-aminomethyl pyridine with 2-pyridine carboxaldehyde derivatives followed by reduction with hydrides, and subsequent action of a second equivalent of 2-pyridine carboxaldehyde derivative; (ii) the condensation of 2-halomethyl-substituted pyridines with primary amines (2-aminomethyl pyridine), with secondary amines (bis(2-pyridylmethyl)amine [DPA]) or with *in situ* generated ammonia. The choice of the 2-halomethyl pyridine method was dictated by the unavailability of 6-iodo-2-pyridinecarboxaldehyde, whereas the preparation of 2-iodo-6-methylpyridine had already been reported [31]. We thus prepared 2-iodo-6-methylpyridine from the 2-bromo-6-methylpyridine precursor, and obtained upon radical bromination reaction the 2-(bromo-methyl)-6-iodopyridine, as the source of iodo pyridine in our ligands.



Scheme 1. Synthetic pathways for ligands I_nTPA . Conditions: (i): TMSCl , NaI , 100°C , 4 days, propionitrile (according to Ref. [31]); (ii): NBS , Benzoyl peroxide 4%, 90°C , 5 h, CCl_4 ; (iii): DPA , NaHCO_3 , EtOH , 90°C , 16 h; (iv): 2-aminomethyl pyridine, Na_2CO_3 , EtOH , 90°C , 16 h; (v): $\text{NH}_4\text{Cl}/\text{NaOH}$ (pH 10), $\text{THF}:\text{H}_2\text{O}$ 90:10, 4 days, R.T.

The synthesis of ligands turned out to be straightforward, as shown in Scheme 1, although a moderate yield of 30% only in analytically pure compound could be obtained for I₂TPA. All tripods displayed good stability, and were characterized by ¹H NMR and elemental analyses. The metalation reactions were carried out following already reported procedures [8,28], and afforded the complexes I₁TPAFeCl₂, I₂TPAFeCl₂ and I₃TPAFeCl₂ as yellow-orange, yellow and pale yellow solids, with yields of 85–90%. Although oxygen-sensitive, the complexes turned out to be thermally stable when stored under inert atmosphere.

In UV–Vis spectroscopy, I₁TPAFeCl₂ exhibited the expected MLCT absorption for high-spin complexes at $\lambda = 375$ nm, with a molecular extinction coefficient $\varepsilon = 1.0 \times 10^3 \text{ mol}^{-1} \text{ L cm}^{-1}$ supporting coordination of the three pyridines of the tripod. By contrast, the similar MLCT absorption was found at $\lambda = 370$ nm ($\varepsilon = 0.5 \times 10^3 \text{ mol}^{-1} \text{ L cm}^{-1}$) for I₂TPAFeCl₂ and non-existent with I₃TPAFeCl₂. The weak (half-reduced with respect to I₁TPAFeCl₂) intensity for the former and the absence of transition for the latter indicate a hypodentate coordination mode of the ligand around the metal [28,32]. All data are shown in the Supplementary Content section. The molecular conductivity values were found to be $\Lambda = 19.2, 23.1, 15.3 \text{ S cm}^2 \text{ mol}^{-1}$, for I₁TPAFeCl₂ (3.7 mM), I₂TPAFeCl₂ (3.4 mM) and I₃TPAFeCl₂ (1.0 mM), respectively, indicating limited dissociation in solution.

The ¹H NMR spectra of all three complexes displayed paramagnetically shifted signals, indicating a high-spin state of Fe(II) in these complexes. The spectrum of I₁TPAFeCl₂, recorded in CH₃CN exhibited well-defined signals. It looks very similar to that of the already published BrTPAFeCl₂ [28], with $\delta_{\alpha\text{-H}} = 117$ ppm ($\Delta_{\nu 1/2} = 553$ Hz), $\delta_{\text{CH}_2} = 65$ ppm ($\Delta_{\nu 1/2} = 608$ Hz), 57 ppm ($\Delta_{\nu 1/2} = 352$ Hz) and 42 ppm ($\Delta_{\nu 1/2} = 521$ Hz), $\delta_{\text{py}} = 51$ ppm ($\Delta_{\nu 1/2} = 40$ Hz) and 46 ppm ($\Delta_{\nu 1/2} = 42$ Hz), $\delta_{\text{py-1}} = 28$ ppm ($\Delta_{\nu 1/2} = 87$ Hz) and 18 ppm ($\Delta_{\nu 1/2} = 150$ Hz), and $\delta_{\gamma\text{py}}$ and $\delta_{\gamma\text{py-1}} = 10$ ppm ($\Delta_{\nu 1/2} = 28$ Hz) and 8 ppm ($\Delta_{\nu 1/2} = 24$ Hz). No tractable signals could be observed in the diamagnetic region, between +10 and –10 ppm.

By contrast, I₂TPAFeCl₂ exhibited a poorly defined spectrum with broader resonances at $120 < \delta < 20$ ppm with $920 < \Delta_{\nu 1/2} < 100$ Hz. Zooming the spectrum into the diamagnetic region allowed detection of resonances assigned to the uncoordinated iodo-pyridine. Finally, the poor solubility of I₃TPAFeCl₂ precluded any observation of ¹H NMR signals, even when CD₃NO₂ was used instead of CD₃CN. All NMR data are displayed in the Supplementary content.

We already know that the presence of poorly resolved signals in the ¹H NMR spectrum, or even the lack of signals, together with a weak MLCT signal in UV–Vis, correlate with a trigonal bipyramidal geometry (TBP) around the metal centre [8,25,28,32] in FeCl₂ complexes.

The cyclic voltammetry can sometimes be informative with respect to the geometry around the metal: when observed at moderate positive potential ($150 < E_{1/2} < 300$ mV/SCE), reversible Fe(II)/Fe(III) waves indicate the presence of LFeCl₂ complexes with the usual octahedral geometry: this is the case for TPAFeCl₂, Me₁TPA-

FeCl₂ and [C₆H₄(OMe)₂]₁TPAFeCl₂ [10,33]. The trigonal bipyramidal geometries generally afford lower values of the potentials, in line with hypodentate coordination of the ligand: this is the case with [C₆H₄(OMe)₂]₃TPAFeCl₂ with $E_{1/2} = 9$ mV/SCE [10], [C₆H₄(OH)₂]₂-TPAFeCl₂ with $E_{1/2} = 10$ mV/SCE [35].

In the present study the Fe(II)/Fe(III) couple of I₁TPAFeCl₂ is measured at $E_{1/2} = 210$ mV/SCE, whereas I₂TPAFeCl₂ and I₃TPAFeCl₂ exhibit pseudo reversible waves at $E_{1/2} = 44$ and 54 mV/SCE, respectively. Thus the $E_{1/2}$ value for I₁TPAFeCl₂ falls into the expected range of potentials for octahedral complexes, whereas the values found for both other complexes support hypodentate coordination and trigonal bipyramidal geometries. The data are displayed in the Supplementary Content section.

Considering all the above-mentioned data, we reached the conclusion that in solution, the complexes of the present study display the geometry indicated in Scheme 2.

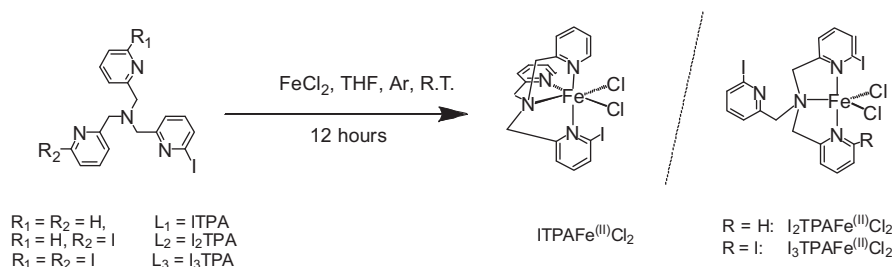
Slow diffusion of diethyl ether in an acetonitrile (I₁TPAFeCl₂) or methylene chloride (I₂TPAFeCl₂) solution afforded single crystals, suitable for structural determination. For these two compounds, the geometry as observed in the solid state perfectly matches that postulated in solution from the spectroscopic studies.

In general, in complexes with single-substituted ligands, a distorted octahedral geometry is observed, and the substituted pyridine lies in lateral position (i.e. the unsubstituted pyridines lie in the cis position to each other) to minimize the steric intramolecular repulsions [8,9,28,33]. Complex I₁TPAFeCl₂ is not exception to this fact.

I₁TPAFeCl₂ crystallizes with two molecules in the asymmetric unit. Although displaying a similar geometry, these two molecules termed I₁TPAFeCl₂ (a) and I₁TPAFeCl₂ (b) slightly differ in terms of equatorial distortion. The ORTEP diagram of the (b) form is displayed in Fig. 1.

Both forms share common features such as a strongly distorted octahedral geometry, with $\angle \text{N}_{\text{amine}}\text{FeN}_{\text{pyridine}}$ angles never reaching more than 78° as expected for a five-membered metallacycle, slightly open $\angle \text{Cl1FeCl2}$ angles (96.5° and 95.2°), and relatively long metal to pyridine distances with the shortest one being not less than 2.18 Å. All these data support high-spin state of the metal in this complex.

Complex I₁TPAFeCl₂ (a) is the low distorted form. The shortest metal to pyridine distance is dFeN3 = 2.19 Å, i.e. the one involving coordination of the axial pyridine. The longest one is dFeN4 = 2.40 Å, clearly indicating noticeable elongation due to repulsive interaction between the iodine atom in α position of the pyridine, and the equatorial chloride ion. This value represents one of the highest ones among all already obtained data for similar compounds. In complexes with α -substituted ligands, the axial deformation is quantified by the α angle between the plane defined by the Cl1–Fe–Cl2 atoms and the mean plane of the axial pyridine [33]. In the present case, the deformation is significant – yet not extreme – with $\alpha = 13.2^\circ$. The equatorial distortion is expressed by the trans-equatorial distortion parameter ρ obtained as the product of the dihedral angle ϕ between the trans equatorial



Scheme 2. Ligands and complexes reported in this study.

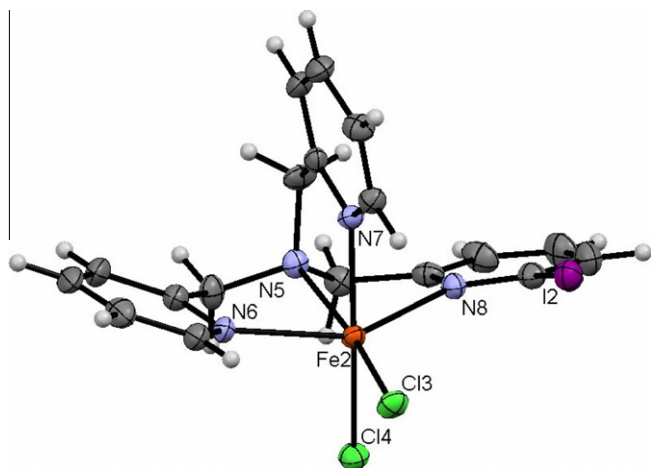


Fig. 1. ORTEP diagram of $I_1TPAFcCl_2$ (b) showing a partial numbering scheme, and structural parameters. Selected bond distances (Å) and angles ($^\circ$): Fe2–N5 = 2.275 (4), Fe2–N6 = 2.246 (3), Fe2–N7 = 2.178 (3), Fe2–N8 = 2.342 (3), Fe2–Cl3 = 2.3515 (11), Fe2–Cl4 = 2.4677(12), $\angle N5Fe2Cl3 = 169.07$ (10), $\angle N6Fe2N8 = 145.34$ (13), $\angle N7Fe2Cl4 = 167.38$ (10), $\angle Cl3Fe2Cl4 = 95.24$ (4), $\angle N6Fe2N5 = 75.10$ (13), $\angle N8Fe2N5 = 71.03$ (13), $\angle N7Fe2N5 = 77.42$ (13).

pyridines, and the torsion angle between the planes of the two trans equatorial pyridines, θ [8,33]. In the present case, and in a paradoxical way, the mechanical effect of the elongation of the Fe–N4 bond is to unstress the coordination polyhedron around the metal: as a consequence, the value of the dihedral angle

between the two equatorial pyridines remains low, and $\rho = 52.1^\circ$ indicates only moderate trans-equatorial distortion.

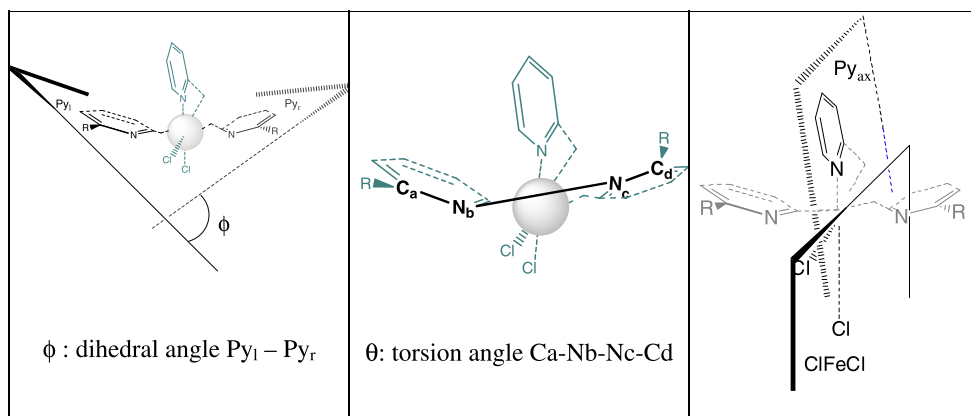
Complex $I_1TPAFcCl_2$ (b) is the high distorted form. Here also, the shortest metal to pyridine distance is the one involving coordination of the axial pyridine, with $dFe2N7 = 2.18$ Å. The longest one is that between the metal and the iodo pyridine, with $dFe2N8 = 2.34$ Å. This value is significantly shorter than the corresponding one in the low distorted form. As a consequence and to minimize steric interaction with the coordinated chloride ions, the dihedral angle ϕ is more pronounced, and in the end trans-equatorial distortion increases with $\rho = 84.3^\circ$.

The equatorial distortion parameters of both (a) and (b) forms are given in Fig. 2.

Fig. 3 shows the ORTEP diagram of compound $I_2TPAFcCl_2$. The iron lies in a distorted TBP geometry: one of the two iodo-pyridines of the tripod has decoordinates. As indicated above in $I_1TPAFcCl_2$, $dFeN4 = 2.40$ Å i.e. already noticeably elongated; obviously, coordination of a second iodo-pyridine in a $FeCl_2$ complex would result in an unacceptable distortion: thus, TBP geometry is the obvious solution for $I_2TPAFcCl_2$.

The longest metal to nitrogen distance is still the one involving coordination of the iodo-pyridine, with however a shorter value: $dFeN3 = 2.25$ Å. The shortest metal to nitrogen bond is the one corresponding to coordination of the amine, with $dFeN1 = 2.17$ Å. Here again, these data support high-spin state of the metal centre in this complex.

The value of the $\angle Cl_1FeCl_2$ angle is for complexes with TBP geometry a good indication of the steric stress around the metal.



I ₁ TPAFcCl ₂ (a)		
7.9	6.6	α = 13.2 °
ρ = ϕ * θ = 52.1 ° ²		

I ₁ TPAFcCl ₂ (b)		
28.4	3.0	α = 11.3 °
ρ = ϕ * θ = 84.3 ° ²		

Fig. 2. Axial and trans equatorial distortion parameters in both (a) and (b) forms of $I_1TPAFcCl_2$.

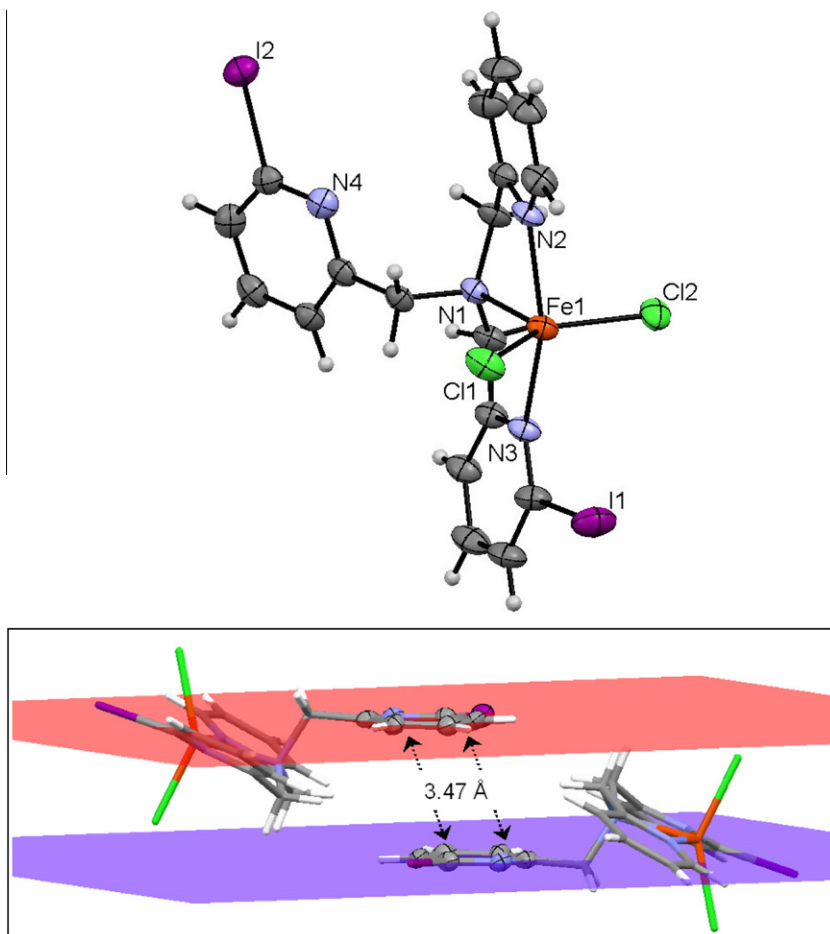


Fig. 3. ORTEP diagram of $I_2TPAFeCl_2$ showing a partial numbering scheme. Selected bond distances (Å) and angles ($^\circ$): Fe1–N1 = 2.170 (5), Fe1–N2 = 2.194 (5), Fe1–N3 = 2.253 (5), Fe1–Cl1 = 2.2883 (18), Fe1–Cl2 = 2.3258 (18). $\angle N3Fe1N2 = 154.9$ (2), $\angle N1Fe1Cl1 = 116.47$ (14), $\angle N1Fe1Cl2 = 100.69$ (14), $\angle Cl1Fe1Cl2 = 142.84$ (8). Focus on two adjacent molecules within the unit cell, showing π -stacking effects between two dangling iodopyridines.

In general, relatively invariant values lying in the $130^\circ < [\angle Cl_1FeCl_2] < 135^\circ$ range are found [10,25,28,33]. In the present case $\angle Cl_1FeCl_2 = 142.8^\circ$, which is the largest value found for $FeCl_2$ complexes with simple ligands,² higher than the value of 130.7° reported in the $Br_2TPAFeCl_2$ analogue [28]. This clearly reflects the steric effect of the iodine atom around the metal centre.

An other striking feature of this structure is the particular stacking of the two adjacent molecules within the unit cell. The dangling iodopyridine of one complex is coplanar to that of its neighbour, as seen in Fig. 3, and both strongly interact with each other, with an interplanar distance of 3.47 Å. This represents an academic example of π -stacking effect [34]. Thus, in the solid state the structure of the complex can be seen as the non-covalent association of two monomers of $I_2TPAFeCl_2$. This is in strong contrast with the structure of the $Br_2TPAFeCl_2$ analogue [28].

In conclusion, we reported in this communication the easy synthesis of the three α -iodo substituted tripods in the tris(2-pyridylmethyl)amine series, the preparation of which was so far unpublished. The dichloroferrous complexes are stable compounds, and X-ray crystal analysis definitely evidences the important steric hindrance due to the presence of bulky substituents, and the tendency of the dangling iodopyridine to aggregate. Future studies should shed light on the utility of such ligands in the

control of the ligand field properties within various metal-containing complexes.

Acknowledgements

We thank the CNRS, the Université Louis Pasteur and the Université de Strasbourg. The Institut de Chimie de Strasbourg is also gratefully acknowledged. We also thank all the colleagues from the Service de Diffraction des Rayons X, the Service de Micro-analyse, and the Service de Spectrométrie de Masse of the Institut de Chimie de Strasbourg.

Appendix A. Supplementary material

CCDC 774440 and 774439 (I_2FeCl_2) contains the supplementary crystallographic data for $I_1TPAFeCl_2$ and I_2FeCl_2 . These data can be obtained free of charge from The Cambridge Crystallographic Data Centre via http://www.ccdc.cam.ac.uk/data_request/cif. Supplementary data associated with this article can be found, in the on-line version, at doi:10.1016/j.ica.2010.10.024.

References

- [1] A.G. Blackman, *Eur. J. Inorg. Chem.* (2008) 2633.
- [2] A.G. Blackman, *Polyhedron* 24 (2005) 1.
- [3] L.M. Berreau, *Comments Inorg. Chem.* 28 (2007) 123.
- [4] M. Costas, K. Chen, L. Que Jr., *Coord. Chem. Rev.* 200–202 (2000) 517.
- [5] M. Costas, M.P. Mehn, M.P. Jensen, L. Que Jr., *Chem. Rev.* (2004) 939.

² An exceptionally high value of $\angle Cl_1FeCl_2 = 152.6^\circ$ was found in a $FeCl_2$ complex with a tris(2-aryl substituted) ligand, as the results of intramolecular interaction of the substituents of the ligand. See Ref. [10].

- [6] S.V. Kryatov, E.V. Rybak-Akimova, S. Schindler, *Chem. Rev.* 105 (2005) 2175.
- [7] Y.V. Korendovych, S.V. Kryatov, E.V. Rybak-Akimova, *Acc. Chem. Res.* 40 (2007) 510.
- [8] N.K. Thallaj, O. Rotthaus, L. Benhamou, N. Humbert, M. Elhabiri, M. Lachkar, R. Welter, A.-M. Albrecht-Gary, D. Mandon, *Chem. Eur. J.* 14 (2008) 6742.
- [9] A. Wane, N.K. Thallaj, D. Mandon, *Chem. Eur. J.* 15 (2009) 10593.
- [10] L. Benhamou, A. Machkour, O. Rotthaus, M. Lachkar, R. Welter, D. Mandon, *Inorg. Chem.* 48 (2009) 4777.
- [11] N.K. Thallaj, J. Przybilla, R. Welter, D. Mandon, *J. Am. Chem. Soc.* 130 (2008) 2414.
- [12] Y. Zang, J. Kim, Y. Dong, E.C. Wilkinson, E.H. Appelman, L. Que Jr., *J. Am. Chem. Soc.* 119 (1997) 4197.
- [13] B. Li, W.R.-J. Wie, J. Tao, R.-B. Huang, L.-S. Zheng, Z. Zheng, *J. Am. Chem. Soc.* 132 (2010) 1558.
- [14] M. Nihei, M. Ui, H. Oshio, *Polyhedron* 28 (2009) 1718.
- [15] I. Boldog, F. Munoz-lara, A.-B. Gaspar, M.C. Munoz, M. Seredyuk, J.-A. Real, *Inorg. Chem.* 48 (2009) 3710.
- [16] S.R. Batten, J. Bjernemose, P. Jensen, B.A. Leita, K.S. Murray, B. Moubaraki, J.P. Smith, H. Toftlund, *Dalton Trans.* 20 (2004) 3370.
- [17] K.S. Min, A.G. Di Pasquale, A.N. Rheingold, H.S. White, J.S. Miller, *J. Am. Chem. Soc.* 131 (2009) 6229.
- [18] C. Enachescu, C.A. Hauser, J.-J. Girerd, M.-L. Boillot, *Chem. Phys. Chem.* 7 (2006) 1127.
- [19] E. Collet, M.-L. Boillot, J. Herbert, N. Moisan, M. Servol, M. Lorenc, L. Toupet, M. Buron-Le Coite, A. Tissot, J. Sainton, *Acta Crystallogr., Sect. B: Struct. Sci.* B65 (4) (2009) 474.
- [20] G. Anderegg, F. Wenk, *Helv. Chim. Act.* 50 (1967) 2330.
- [21] M.S. Nelson, J. Rodgers, *J. Chem. Soc. (A)* 1 (1968) 272.
- [22] J. Romary, R.D. Zachariasen, J.D. Barger, H. Schiesser, *J. Chem. Soc. (C)* 23 (1968) 2884.
- [23] M.M. Da Mota, J. Rodgers, S.M. Nelson, *J. Chem. Soc. (A)* 1 (1969) 2036.
- [24] C.L. Chuang, O. dos Santos, X. Xu, J.W. Canary, *Inorg. Chem.* 36 (1997) 1967.
- [25] A. Machkour, D. Mandon, M. Lachkar, R. Welter, *Inorg. Chem.* 43 (2004) 1545.
- [26] W.L.F. Armarego, D.D. Perrin, *Purification of Laboratory Chemicals*, fourth ed., Pergamon Press, Oxford, 1997.
- [27] R. Adams, S. Miyano, *J. Am. Chem. Soc.* 76 (1954) 3168.
- [28] D. Mandon, A. Machkour, S. Goetz, R. Welter, *Inorg. Chem.* 41 (2002) 5363.
- [29] *Kappa CCD Operation Manual*, B.V. Nonius, Delft, The Netherlands, 1997.
- [30] G.M. Sheldrick, *SHELX97*, Program for the Refinement of Crystal Structures, University of Göttingen, Germany, 1997.
- [31] M. Schlosser, F. Cottet, *Eur. J. Org. Chem.* (2002) 4181.
- [32] A. Machkour, D. Mandon, M. Lachkar, R. Welter, *Inorg. Chim. Acta* 358 (2005) 339.
- [33] L. Benhamou, M. Lachkar, D. Mandon, R. Welter, *Dalton Trans.* 1 (2008) 6996.
- [34] A.L. Speck, *J. Appl. Crystallogr.* 36 (2003) 7.
- [35] A. Machkour, N.K. Thallaj, L. Benhamou, M. Lachkar, D. Mandon, *Chem. Eur. J.* 12 (2006) 6660.